Journal of Applied Mathematics and Computation (JAMC), 2019, 3(4), 599-605
http://www.hillpublisher.com/journals/JAMC
ISSN Online: 2576-0645
ISSN Print: 2576-0653

Gauss – Seidel numerical study of 2D incompressible symmetric viscous flow in a closed rectangular C section channel

Jacob Nagler

School of Mechanical Engineering, University of Tel-Aviv, Tel-Aviv 69978, Israel

How to cite this paper: Nagler J. (2019) Gauss – Seidel numerical study of 2D incompressible symmetric viscous flow in a closed rectangular C section channel. *Journal of Applied Mathematics and Computation*, **3(4)**, 599-605.

DOI: 10.26855/jamc.2019.06.001

***Corresponding author:** Jacob Nagler, School of Mechanical Engineering, University of Tel-Aviv, Tel-Aviv 69978, Israel.

Email: syankitx@Gmail.com

Abstract

In this paper, numerical simulation based on generalized Gauss-Seidel method (which is also known as theta method) was performed in case of a 2D incompressible symmetric viscous flow in a closed rectangular C section channel along with no-slip boundary conditions on the walls. Also, model calibration was involved during numerical simulation model. Comparisons between other numerical studies and current study have been found to adjust qualitatively.

Keywords

Gauss - Seidel, 2D, rectangular C section, viscous flow

1. Introduction

Numerical simulations of viscous fluid flow in ducts, pipes and channels are an important subject in fluid mechanics field. The case of an arbitrary sections is a unique sub-category of ducts simulation and was investigated lately by Fukuchi [1- 4] and others [5-10].

In this essay, Gauss – Seidel numerical method application will be demonstrated in case of 2D incompressible symmetric potential viscous flow in a closed rectangular C section channel with no-slip boundary conditions on the walls. Two-dimensional momentum (partial differential) elliptic equation (PDE) with constant coefficients has been solved numerically in Cartesian axes similarly to [11, 12].

Finally, comparison between other numerical solutions will be presented and compared together with other studies.

2. Flow field equations

Consider a steady-state fluid that moves in a rectangular C section shaped channel as appear in the scheme below (Fig. 1):

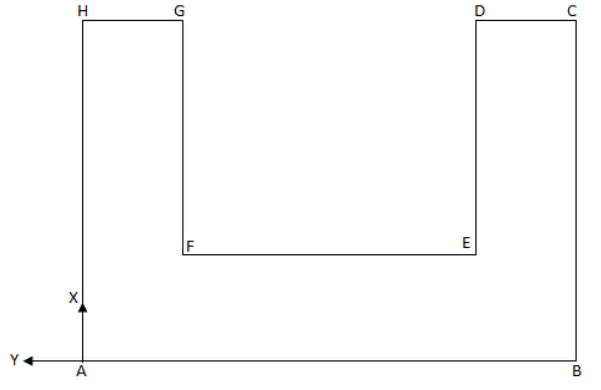

Fig.1 2D viscous fluid model in C section shaped channel.

The fluid velocity function $\varphi(x,y)$ is dependent on the Cartesian axes x,y while the fluid viscosity and the pressure gradient are constants (assumption), and will be noted by μ,c, respectively.

The partial differential equation, which describes the change in the velocity profile distribution that flows in a constant state, is:

$$\frac{\partial^2\varphi}{\partial x^2}+\frac{\partial^2\varphi}{\partial y^2}=-\frac{c}{\mu} \tag{1}$$

During the problem we will use the following values for the pressure gradient and viscosity: $c = 0.0002[lb/in^2/in]$, $\mu = 0.25\bullet 10^{-5}[lb\bullet \sec/in^2]$. One step before solving (1), we will present the boundary conditions (b.c.). Assuming no-slip b.c. on the wall (ACBCDEFGHA) in the case of the viscous fluid, yields:

$$\varphi(AB)=\varphi(BC)=\varphi(CD)=\varphi(DE)=\varphi(EF)=\varphi(FG)=\varphi(GH)=\varphi(HA)=0 \tag{2}$$

Moreover, we will assume that the wall geometry values are:

$$AB=BC=AH=6[inch]\ ;\ CD=DG=GH=2[inch]\ ;\ DE=FG=4[inch] \tag{3}$$

3. Numerical methods formulation

Numerical solution procedure for solving elliptic equation with constant coefficients has been studied by [1-8]. Finite difference method formulation yields the following numerical algebraic equation:

$$\frac{\varphi_{i+1,j}-2\varphi_{i,j}+\varphi_{i-1,j}}{\delta x^2}+\frac{\varphi_{i,j+1}-2\varphi_{i,j}+\varphi_{i,j-1}}{\delta y^2}=-\frac{c}{\mu}=const\ , \tag{5}$$

while $(x,y)\rightarrow(i,j)$ and δx, δy are the step size in the specified direction, respectively.

Since $AH = BC = 6[ins]$ then $0 \le x \le 6$ and $1 \le i \le M + 2$, where $\delta x = \frac{6}{M+1}$ and M symbols the number of points in the x direction. In similar way, $AB = 6[ins]$ such as $0 \le y \le 6$ and $1 \le j \le N + 2$, where $\delta y = \frac{6}{N+1}$ and M symbols the number of points in the Y direction.

In order to solve the Eq. (5), we will use the Gauss- Seidel method due to its relatively (to Jacobi method) small iterations number by updating the arrays & indexes and also its fast convergent. Now, the inner points will be expressed by the finite difference method with some arrangement while iterations number will be represented by the n index:

$$\varphi_{i,j}^{\ n+1}=\frac{\delta y^2(\varphi_{i+1,j}^{\ \ n}+\varphi_{i-1,j}^{\ \ n+1})+\delta x^2(\varphi_{i,j+1}^{\ \ n}+\varphi_{i,j-1}^{\ \ n+1})-\delta x^2\delta y^2 f}{2(\delta x^2+\delta y^2)} \tag{6}$$

The sections inner points in the X, Y directions are expressed by the following range:

$$\begin{cases} 2\le j\le\frac{(N+1)}{3},\ 2\le i\le M+1 \\ \frac{(N+1)}{3}+2\le j\le\frac{2(N+1)}{3},\ 2\le i\le\frac{(M+1)}{3} \\ \frac{2(N+1)}{3}+2\le j\le N+1,\ 2\le i\le M+1 \end{cases} \tag{7}$$

The solution procedure that was implemented in MATLAB program is as follows:

1. Assuming the initial guess.
2. Iterative solution for the inner points in the range section (7).
3. If the iteration convergent conditionfalsedoes not fulfill, the program return to stage 1.

Next, three methods which are derived from Eq. (5), will be discussed here.

4. Gauss- Seidel Numerical method parameters influence

Parameters analysis was including the following parameters examination:

- δx
- δy
- ε
- Initial Guess

However, after examining Run-Time for convergence, number iterations for convergence and the minimal error, we have obtained the following values:

- Number of step in the x – axis: M = 59 $\rightarrow$ δx = 0.1 as derived from Table 1.
- Number of step in the y – axis: N = 59 $\rightarrow$ δy = 0.1 as derived from Table 2.
- Convergence criteria is: $\varepsilon = 1 \cdot 10^{-3}$ as derived from Table 3 as derived from Table 3.
- Initial Guess is matrix of ones as derived from Fig. 2 (a)-(b) (has no influence on convergence).

Table 1. Convergence parameters for varying δx step parameter.

Initial Guess	N	M	Number of iterations	Run-Time [sec]	δy	δx
ones(*N*+2, *M*+2)	59	29	645	1.17	0.1	0.2
ones(*N*+2, *M*+2)	59	59	993	4.43	0.1	0.1
ones(*N*+2, *M*+2)	59	83	1419	9.98	0.1	$\frac{1}{14}$
ones(*N*+2, *M*+2)	59	113	2119	24.35	0.1	$\frac{3}{56}$

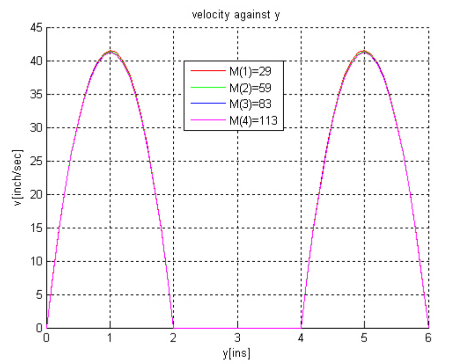

$$R_{M=113,29} = \frac{41.54-41.2}{41.2}\cdot 100 \simeq 0.83\%$$

$$R_{M=113,59} = \frac{41.2-41.32}{41.2}\cdot 100 \simeq 0.29\%$$

$$R_{M=113,83} = \frac{41.25-41.2}{41.2}\cdot 100 = 0.12\%$$

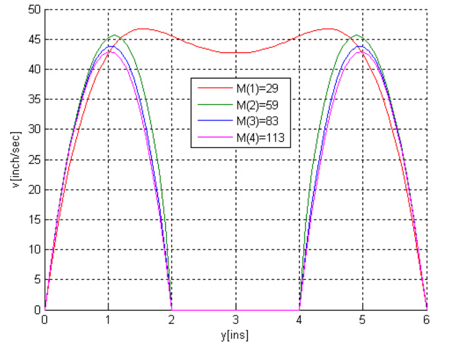

$$R_{M=113,29} = \left|\frac{42.94-46.77}{42.94}\right|\cdot 100 = 8.92\%$$

$$R_{M=113,59} = \left|\frac{42.94-45.66}{42.94}\right|\cdot 100 = 6.33\%$$

$$R_{M=113,83} = \left|\frac{42.94-43.84}{42.94}\right|\cdot 100 = 2.1\%$$

Table 2. Convergence parameters for varying δx step parameter.

Initial Guess	N	M	Number of iterations	Run-Time [sec]	δy	δx
$ones(N+2, M+2)$	59	29	645	0.89	0.1	0.2
$ones(N+2, M+2)$	59	59	992	2.37	0.1	0.1
$ones(N+2, M+2)$	59	83	1418	4.99	0.1	$\frac{1}{14}$
$ones(N+2, M+2)$	59	113	2118	19.42	0.1	$\frac{3}{59}$

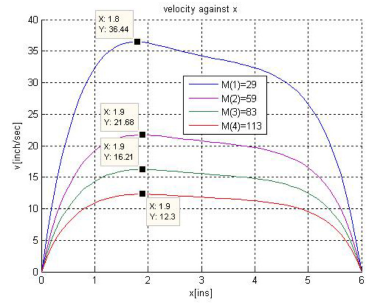

$$R_{N=113,29} = \left|\frac{16.21-12.3}{12.3}\right| \cdot 100 = 31.8\%$$

$$R_{N=113,59} = \left|\frac{21.68-12.3}{12.3}\right| \cdot 100 = 76.26\%$$

$$R_{N=113,83} = \left|\frac{36.44-12.3}{12.3}\right| \cdot 100 = 196.26\%$$

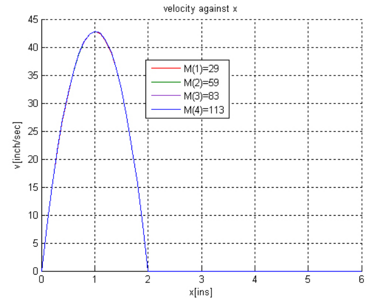

$$R_{N=113,29} = \frac{42.85-42.78}{42.85} \cdot 100 = 0.163\%$$

$$R_{N=113,59} = \frac{42.85-42.83}{42.85} \cdot 100 = 0.047\%$$

$$R_{N=113,83} = \frac{42.85-42.84}{42.85} \cdot 100 = 0.023\%$$

Table 3. Convergence parameters for varying ε convergence parameter.

Initial Guess	N	M	Number of iterations	Run-Time [sec]	δy	ε	δy
$ones(N+2, M+2)$	59	59	373	2.4376	10^{-4}	0.1	0.1
$ones(N+2, M+2)$	59	59	176	1.1510	10^{-3}	0.1	0.1
$ones(N+2, M+2)$	59	59	42	0.2831	10^{-2}	0.1	0.1
$ones(N+2, M+2)$	59	59	3	0.0293	10^{-1}	0.1	0.1

Section $x(1,:), v(0.5\cdot M+0.5,:)$

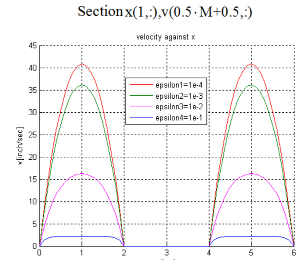

Section $x(1,:), v(M,:)$

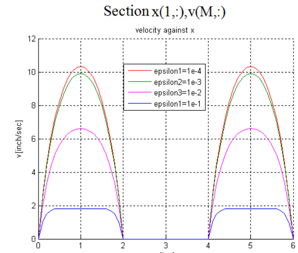

$$R_{\varepsilon=1\cdot10^{-4},1\cdot10^{-3}} = \left|\frac{40.8-36.11}{40.8}\right| \cdot 100 = 11.5\%$$

$$R_{\varepsilon=1\cdot10^{-4},1\cdot10^{-2}} = \left|\frac{40.8-16.21}{40.8}\right| \cdot 100 = 60.3\%$$

$$R_{\varepsilon=1\cdot10^{-4},1\cdot10^{-1}} = \left|\frac{40.8-2.2}{40.8}\right| \cdot 100 = 94.6\%$$

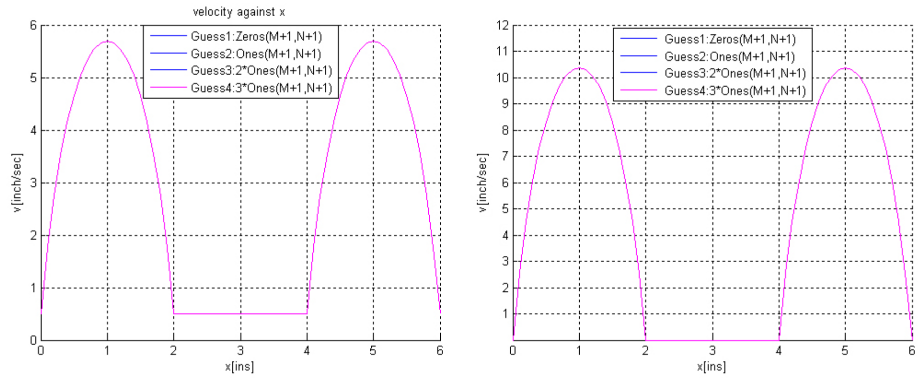

Fig. 2 a. Initial guess influence on convergence in section x(1,:), v(0.5·M+0.5,:).
b. Initial guess influence on convergence in section x(1,:), v(M.:).

5. Numerical results and comparison

In this section, 2D velocity numerical results solution of the second order equation (1) will be presented for the previous section specific parameters in (x, y) coordinates.

As a result of the b.c. that are based on the channel geometry, the 2D velocity is described in Fig. 3 (a) – (b). It seems that the velocity is obtained the maximum value far from the walls (red color). On the other hand the minimal velocity is obtained in the wall section (blue color) due to the no-slip conditions. Also, there are intersection corners (or points) which causes to higher velocity values (peak).

One may observe in Figs. 4(a-b) that the maximum velocity value in the x-axis (at $x = 1.3[ins]$) for y section (at $y = 1.4[ins]$) is $v = 48.98[\frac{inch}{sec}]$ (red color) while the minimal velocity is $v = 48.98[\frac{inch}{sec}]$ at $x = 5.9[ins]$, $y = 1[ins]$ (blue color).

Note that at about y=3 we have symmetry behavior due to symmetric channel geometry along the appropriate boundary conditions. Also, the obtained velocity profile is parabolic and contains local maximum and minimum velocity values including global maximum and minimum values (in the corners).

Additionally, examination of the flow velocity in three 2D sections in the x – axis direction is appear below in Table 4, in relative to the maximum global velocity value ($v = 48.98[\frac{inch}{sec}]$) using Fig. 5 (a)-(c).

Finally, qualitative comparison between current numerical and literature solutions [4], done by Fukuchi [4] shows qualitative agreement (compare Fig.1(a), Fig. 7(a), Fig. 8(a), Fig. 9(a) and Fig.10(a) with our velocity distribution plots).

Table 4. Maximum velocity estimation in chosen section.

Section	Maximum velocity	Relative difference to the global maximum velocity
$X(1, :), v(0.5\cdot(M) - 8.5, :)$	$45.66[\frac{inch}{sec}]$	$\left\lvert\frac{48.98 - 45.66}{48.98}\right\rvert \cdot 100 \approx 6.78\%$
$X(1, :), v(1{:}\ 61, N\text{-}1)$	$21.68[\frac{inch}{sec}]$	$\left\lvert\frac{48.98 - 21.68}{48.98}\right\rvert \cdot 100 \approx 55.73\%$
$X(1, :), v(1{:}\ 61, 0.5\cdot M + 0.5)$	$42.83[\frac{inch}{sec}]$	$\left\lvert\frac{48.98 - 42.83}{48.98}\right\rvert \cdot 100 \approx 12.56\%$

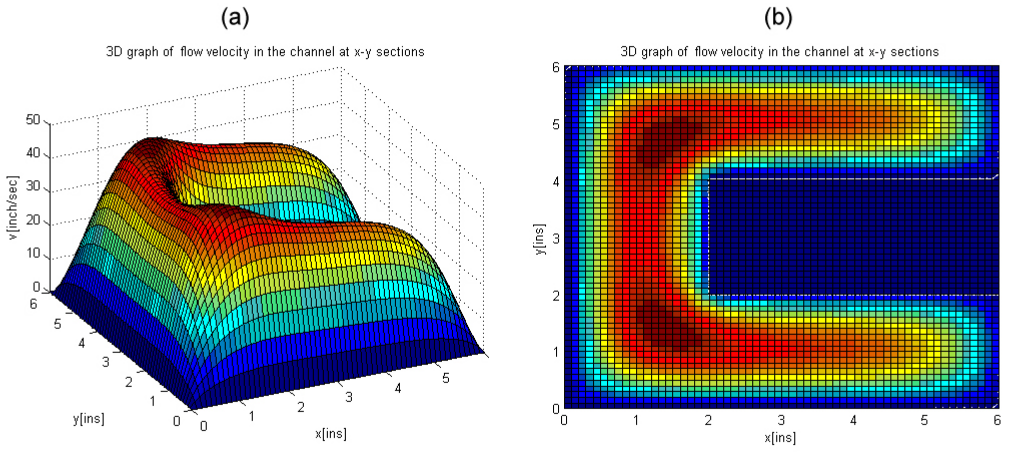

Fig. 3 a. 3D Isometric view of the flow in the channel; b. Channel flow in *x*-*y* section view.

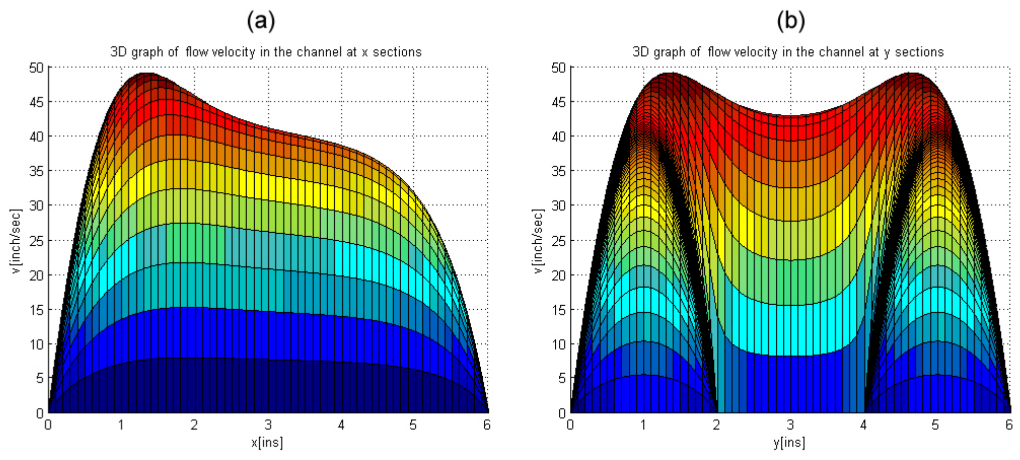

Fig. 4 a. 3D flow section view in the *x* direction; b. 3D flow section view in the *y* direction.

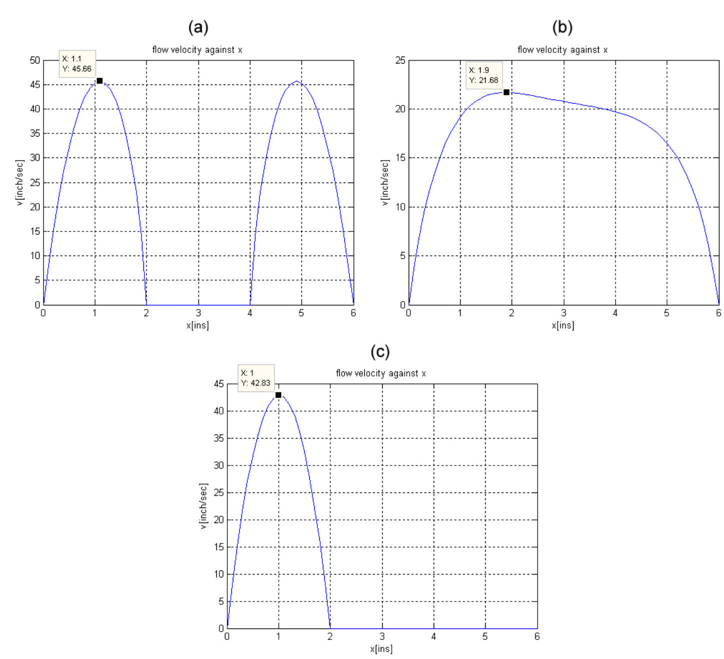

Fig. 5 a. Flow velocity vs. *x* direction for specific *y* sections: *x*(1,:), *v*(0.5·(*M*)-8.5,:); b. Flow velocity vs. *x* direction for specific *y* sections: *x*(1,:), *v*(1:61, *N*-1); c. Flow velocity vs. *x* direction for specific *y* sections: *x*(1,:), *v*(1:61, 0.5·*M*+0.5).

6. Conclusion

This study presents numerical steady-state simulation of planar (2D) viscous fluid flow problem under no-slip conditions inside rectangular C channel represented by elliptic PDE with constants coefficients. The problem of the velocity distribution was solved using the iterative Gauss-Siedel numerical procedure.

Four main optimization numerical parameters were examined for convergent:

- δx step in the x-axis coordinate.
- δy step in the y-axis coordinate.
- ε convergent criterion.
- Initial conditions.

While the test parameters were: Run-Time, iterations number and accuracy. Remark that the optimal initial guess was not influenced by the solution accuracy but only the iterations number and the Run-Time.

Obviously it was found that the problem is symmetric around the section $y = 3$ due to the overall symmetric geometry and the boundary conditions. Also, regions with high velocity (red color) and low velocity (blue color) were obtained. In addition, the maximum and the minimum global velocities value were found to be $v = 48.98[\frac{inch}{sec}]$ and $v = 0[\frac{inch}{sec}]$, respectively. In this context, local regions involved with high and low velocity are exist (especially, near the corner or the walls). Finally, the velocity change is generally parabolic.

Acknowledgements

This study was performed using Prof. Barry Greenberg *Advanced Numerical Analysis* course notes from Technion – Israel Institute of Technology.

References

[1] T. Fukuchi, On convergence process of turbulent shear flows in ducts of rectangular cross-section, 52nd Japan National Congress for Theoretical and Applied Mech.52 (2003)83–90.

[2] T. Fukuchi, Numerical calculation of fully-developed laminar flows in arbitrary cross-sections using finite difference method, *AIP Advances*.(1) (2011) 042109-1.

[3] T. Fukuchi, Numerical stability analysis and rapid algorithm for calculations of fully developed laminar flow through ducts using time-marching method, *AIP Advances*.(3) 032101 (2013).

[4] T. Fukuchi, Numerical analyses of steady-state seepage problems using the interpolation finite difference method, *Soils and Foundations*, 56(4) (2016) 608–626.

[5] T. T. Chandratilleke and T. Nadim, Forced convective heat transfer and fluid flow characteristics in curved ducts, *INTECH*. (2012) 125-150.

[6] D. Xiu and D. M. Tartakovsky, Numerical methods for differential equations is random domains, *SIAM J. Sci. Comput.*, 28 (3) (2006) 1167–1185.

[7] M.R.H. Nobari, A. Nousha and E. Damangir, A numerical investigation of flow and heat transfer in rotating U-shaped square ducts, *Int. J. of Thermal Sci.* 48 (2008) 590–601.

[8] P. Jothiappan, Control of laminar fluid flow and heat transfer in a planar T-channel With rotating obstacle, *J. Phys. Math*. 6 (2) (2015) 1-6.

[9] S. Panahi, H. Ghassemi and H. Nowruzi, Numerical calculations of the potential on the rectangular and elliptic domains with various aspect ratios, *J. of App. Math. and Comp Mech.* 16 (3) (2017) 73-83.

[10] A. M. Sahar, J. Wissink, M. M. Mahmoud and T. G. Karayiannis, M. S. A. Ishak, Effect of hydraulic diameter and aspect ratio on single phase flow and heat transfer in a rectangular micro-channel, *App. Thermal Eng.* (115) (2017) 793–814.

[11] T. Fukuchi, High-order accurate and high-speed calculation system of 1D Laplace and Poisson equations using the interpolation finite difference method, *AIP Advances.* (9) (2019) 055312-1.

[12] P.K. Pandey and S.S.A. Jaboob, A finite difference method for a numerical solution of elliptic boundary value problems, *App. Math. & Nonlinear Sci.* 3(1) (2018) 311–320.